Influence of interface mobility on the evolution of austenite-martensite grain assemblies during annealing

Santofimia Navarro, MJ; Speer, JG; Clarke, AJ; Zhao, L; Sietsma, J

DOI
10.1016/j.actamat.2009.06.024

Publication date
2009

Document Version
Final published version

Published in
Acta Materialia

Available online at www.sciencedirect.com
ScienceDirect
Acta Materialia 57 (2009) 4548–4557
Acta MATERIALIA
www.elsevier.com/locate/actamat

Influence of interface mobility on the evolution of austenite–martensite grain assemblies during annealing

M.J. Santofimia [a,b,*], J.G. Speer [c], A.J. Clarke [d], L. Zhao [a,b], J. Sietsma [b]

[a] Materials Innovation Institute (M2i), Mekelweg 2, 2628 CD Delft, The Netherlands
[b] Department of Materials Science and Engineering, Delft University of Technology, Mekelweg 2, 2628 CD Delft, The Netherlands
[c] Advanced Steel Processing and Products Research Center, Colorado School of Mines, Golden, CO 80401, USA
[d] Materials Science and Technology Division, Mail Stop G770, Los Alamos National Laboratory, Los Alamos, NM 87545, USA

Received 9 March 2009; accepted 17 June 2009
Available online 13 July 2009

Abstract

The quenching and partitioning (Q&P) process is a new heat treatment for the creation of advanced high-strength steels. This treatment consists of an initial partial or full austenitization, followed by a quench to form a controlled amount of martensite and an annealing step to partition carbon atoms from the martensite to the austenite. In this work, the microstructural evolution during annealing of martensite–austenite grain assemblies has been analyzed by means of a modeling approach that considers the influence of martensite–austenite interface migration on the kinetics of carbon partitioning. Carbide precipitation is precluded in the model, and three different assumptions about interface mobility are considered, ranging from a completely immobile interface to the relatively high mobility of an incoherent ferrite–austenite interface. Simulations indicate that different interface mobilities lead to profound differences in the evolution of microstructure that is predicted during annealing.

Keywords: Quenching; Annealing; Steels; Diffusion; Thermodynamics

1. Introduction

Current demands on fuel consumption and safety have led the automotive industry to search for new advanced steels with enhanced strength and ductility. One of the ideas being explored is the development of low-carbon steels with a microstructure consisting of martensite and a considerable fraction of retained austenite. This combination of phases can lead to a high strength, because of the presence of martensite, and considerable formability. Although these microstructures have been observed in the past in quenched martensitic steels, the amount and stability of the retained austenite found were usually low [1,2]. In addition, during subsequent tempering, reduction of carbon in the martensite occurred via carbide precipitation, whereas austenite was usually decomposed into ferrite and carbides.

Knowledge of the effect of some elements, e.g. silicon and aluminum, in inhibiting cementite precipitation has opened the possibility for obtaining carbon-enriched austenite by partitioning of carbon from supersaturated martensite. The recently proposed [3,4] "quenching and partitioning" (Q&P) process makes use of this idea. This new heat treatment consists of a partial martensite transformation (quenching step) from a fully or partially austenitized condition, followed by an annealing treatment (partitioning step) at the same or higher temperature to promote carbon partitioning from the supersaturated martensite to the austenite. During the partitioning step it is intended that the austenite be enriched with carbon, thus allowing its stabilization at room temperature. The

* Corresponding author. Present address: Instituto Madrileño de Estudios Avanzados en Materiales (IMDEA-Materiales), ETS de Ingeniería de Caminos 28040 Madrid, Spain. Tel.: +34 91 549 3422; fax: +34 91 550 3047.
E-mail address: mariajesus.santofimia@imdea.org (M.J. Santofimia).

1359-6454/$36.00
doi:10.1016/j.actamat.2009.06.024

resulting microstructure after the whole thermal cycle consists of ferrite (in the case of an initial partial austenitization), martensite and retained austenite. In this paper, the partitioning step will be further referred to as annealing, to avoid confusion with the process of carbon migration (partitioning).

From the above, it is clear that the essential mechanism of the Q&P process is the transfer of carbon from the supersaturated martensite to the austenite. Given that this mechanism of carbon partitioning was not considered in detail in the past, the conditions under which it takes place are now under debate. Some authors [5–8] have postulated a "constrained carbon equilibrium" (CCE) condition governing the carbon flux from the martensite to the austenite. The CCE takes into account that iron and substitutional atoms are less mobile at temperatures at which carbon diffusion takes place and that the martensite–austenite interface can be assumed immobile or stationary. Therefore, only carbon equilibrates its chemical potential.

There are some experimental observations that question whether the martensite–austenite interface remains stationary during annealing. Zhong et al. [9] have reported the apparent migration of these interfaces in a low-carbon steel after annealing at 480 °C. Although the direction of migration has not been established, this observation indicates the importance of understanding the transfer of iron atoms in relation to the partitioning of carbon. Another interesting observation that contradicts the simplifying assumption of a stationary interface is the reported expansion of the material during the annealing (partitioning step) observed by dilatometry [10], probably indicating changes in the fractions of phases. However, a definitive explanation of the causes of this expansion is not yet available, since it is unclear if the expansion is a result of the continued growth of already present athermal martensite, the nucleation of new isothermal martensite or bainite reaction [11]. Another interesting unexplained feature is the presence of two peaks in the representation of retained austenite fraction vs. annealing time, which has been attributed to the competition between carbon partitioning and carbide precipitation [12].

Given these contradictions, Speer et al. [13] recently considered the implications of iron atom movement on the evolution of the martensite–austenite interface during annealing. According to that work [13], "the difference in iron potential between the ferrite and the austenite creates a driving force for iron to move from one structure to the other, which is accomplished via migration of the existing interface, assuming that nucleation of new crystals does not occur". Under these considerations, Santofimia et al. [14] quantitatively analyzed the motion of the martensite–austenite interface in a model based on thermodynamics and diffusion, assuming the same chemical potential of carbon in martensite and austenite at the interface and allowing motion of the phase interface when a free-energy difference occurs. Simulations corresponding to a particular realistic microstructure were presented, showing a significant bidirectional movement of the martensite–austenite interface. These calculations were made assuming an activation energy for the migration of iron atoms corresponding to data on austenite to ferrite transformation in steels (140 kJ mol^{-1}) [15,16], which implies the assumption of an incoherent martensite–austenite interface. In principle, the use of this activation energy could seem inconsistent with the well-known semicoherent character of the martensite–austenite interface created during martensite formation [17]. However, a treatment of annealing at the transformation temperature or at higher temperatures (that can be identified as the annealing or partitioning temperature of the Q&P process, typically between 250 and 500 °C) can affect the character and thus the mobility of the martensite–austenite interface. In any case, there is a significant lack of studies in this area. Therefore, the theoretical analysis of phases and carbon behavior during annealing of martensite–austenite microstructures assuming different interface characters is an alternative way to study mechanisms and provide an insight into the above-mentioned experimental observations.

In this work, microstructural evolution during annealing of martensite–austenite grain assemblies has been analyzed by means of a modeling approach that considers the influence of the coupling between martensite–austenite interface migration and the kinetics of carbon partitioning. Assuming that the character of the martensite–austenite interface influences the activation energy for iron migration from one phase to the other, three different activation energies are considered in this study: (i) "infinite" (i.e. immobile interface) which corresponds to CCE conditions; (ii) 140 kJ mol^{-1} from data on the austenite to ferrite transformation involving incoherent interfaces [15,16]; and (iii) a higher value (180 kJ mol^{-1}) which represents an estimated value for semicoherent interfaces. Carbon profiles and volume fraction of phases predicted as a function of the quenching temperature, annealing temperature and martensite–austenite interface mobility are analyzed. For simplicity, carbide precipitation is assumed to be suppressed completely.

2. Model

The interaction between carbon partitioning and interface migration is analyzed using the model presented by Santofimia et al. [14]. Some aspects of this model are reviewed here for a proper understanding of the analysis presented in the following sections.

For modeling purposes, martensite is considered to have a body-centered cubic (bcc) structure supersaturated in carbon, whereas austenite is a face-centered cubic (fcc) phase. The model considers the same chemical potential of carbon in bcc and in fcc at the bcc–fcc interface because of the high atomic mobility of interstitial carbon, which is one of the CCE conditions. This condition is expressed in terms of carbon concentration by Eq. (1) presented in Ref. [14].

The motion of interfaces in a microstructure is a result of the repositioning of atoms from lattice positions in one grain to projected lattice positions in a neighboring grain. At a given temperature, the equilibrium concentrations of carbon in fcc, $x_C^{\text{fcc-eq}}$, and bcc, $x_C^{\text{bcc-eq}}$, are given by the metastable equilibrium phase diagram, excluding carbide formation. If the carbon concentrations at the interface are different from the equilibrium values, the phases will experience a driving pressure, ΔG, for a phase transformation towards the equilibrium phase composition. This local driving pressure is experienced at the interface and results in an interface velocity, v, which is proportional to the driving pressure according to:

$$v = M\Delta G, \tag{1}$$

where M is the interface mobility. In this work, the driving pressure is considered proportional to the difference between the equilibrium concentration of carbon in fcc and the interface carbon concentration in fcc, for which the proportionality factor is calculated from Thermo-Calc [18].

The driving pressure can be positive or negative, depending on the relative difference between the equilibrium carbon content of the austenite and the actual carbon concentration in austenite at the interface. The relationship between the carbon content in the austenite at the fcc–bcc interface, $x_C^{\text{fcc–bcc}}$, and the interface migration behavior, according to the present model, is schematically represented in Fig. 1. If the interface is enriched in carbon relative to equilibrium, then the chemical potential of iron is higher in martensite than in austenite and the driving pressure for the movement of the interface promotes interface migration from the austenite to the martensite (Fig. 1a), whereas the interface would be promoted to move in the opposite direction if the interface is depleted in carbon relative to equilibrium (Fig. 1b).

The interface mobility, which is temperature dependent, can be expressed as a product of a pre-exponential factor and an exponential term:

$$M = M_0 \exp\left(-\frac{Q_M}{RT}\right), \tag{2}$$

where Q_M is the activation energy for iron atom motion at the interface. The pre-exponential factor, M_0, can be expressed as [19]:

$$M_0 = \frac{d^4 v_D}{k_B T}, \tag{3}$$

where d is the average atomic spacing in the two phases separated by the interface in question, v_D is the Debye frequency and k_B is the Boltzmann constant. The value of d has been estimated to be 2.55 Å for a martensite–austenite interface [20].

The diffusion of carbon in martensite and austenite is modeled by solving Fick's second law using a standard finite-difference method [21]. Diffusion coefficients are calculated referring to the carbon content in martensite [22] and austenite [23].

3. Simulation conditions

In order to study the influence of the martensite–austenite interface character on the interaction between carbon partitioning and iron migration during annealing, it is assumed that modifications to the interface character lead to different values of the activation energy for iron migration. This is a reasonable qualitative approximation, since the mobility of a martensite–austenite interface during annealing is related to the coherency of the interface. For example, iron atoms migrate more easily in incoherent interfaces. Although it is now not possible to exactly relate the value of the activation energy to the specific character of the interface, approximations can lead to insightful results, as will be shown in the following sections. In this work, three different activation energies are assumed in the calculations.

3.1. Case 1: infinite activation energy

Using the described model, it is possible to check that a very high value of the activation energy (higher than 300 kJ mol^{-1}) leads to an interface mobility low enough to be considered nonexistent over any reasonable timescale

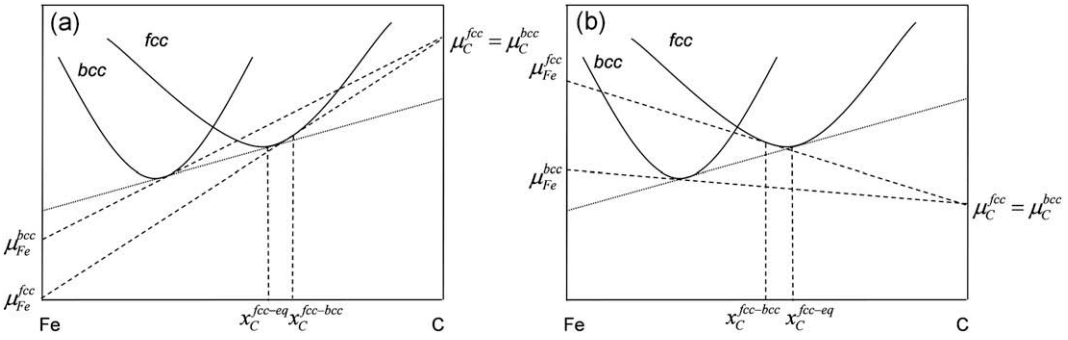

Fig. 1. Schematic diagram illustrating the austenite interface composition under CCE conditions (dashed lines) and under equilibrium (dotted lines). (a) Carbon concentration in the austenite at the interface higher than the equilibrium concentration, and (b) carbon concentration in the austenite at the interface lower than the equilibrium concentration.

(up to days) during annealing at temperatures up to 500 °C. For simplicity, the simulations have been done assuming an infinite value of the activation energy by setting the interface mobility equal to zero. This assumption leads to an immobile interface and to results corresponding to CCE conditions.

3.2. Case 2: $Q_M = 180\ kJ\ mol^{-1}$

An activation energy for iron migration equal to 180 kJ mol^{-1} was selected for this case in order to simulate the situation of limited martensite–austenite mobility, slower than for austenite to ferrite transformations. This value of the activation energy should be considered illustrative for coherent or semicoherent interfaces rather than quantitatively accurate, since currently there is no basis for an accurate estimation of the activation energy for movement of iron atoms at the martensite–austenite interface.

3.3. Case 3: $Q_M = 140\ kJ\ mol^{-1}$

In this case, the activation energy for interface migration was set equal to 140 kJ mol^{-1}, which is the value used by Krielaart and Van der Zwaag in a study on the austenite to ferrite transformation behavior of binary Fe–Mn alloys [15] and by Mecozzi et al. [16] to study the same phase transformation in a Nb microalloyed CMn steel. The resulting mobility can be seen as an upper limit, applying to incoherent interfaces.

Model predictions are sensitive to the alloy used in the calculations. In this work, simulations have been performed assuming a binary Fe–0.25 wt.% C system and a martensite–austenite film morphology (also used in Ref. [14]). The corresponding martensite start temperature (M_s) was calculated to be 433 °C [24]. Simulations considered two annealing temperatures (350 and 400 °C) and different quenching temperatures ranging from 220 to 400 °C. Values of the martensite–austenite interface mobility M, calculated according to Eqs. (2) and (3) for both annealing temperatures studied, are presented in Table 1. Variations in the quenching temperatures lead to different amounts of martensite and austenite prior to annealing. The volume fractions of phases present after the quenching step are estimated by the Koistinen–Marburger equation [25], leading to the values shown in Table 2. The volume fractions of phases present at each quenching temperature and the lath widths of martensite and austenite are related using a "constant ferrite width approach" [26]. This approach is based on the transmission electron microscopy observations of Krauss and co-workers, indicating that most martensitic lath widths range approximately from 0.15 to 0.2 μm [27,28]. Additionally, Marder [29] reported that a lath width of 0.2 μm was most frequently observed for 0.2 wt.% C martensite. Therefore, a constant martensite lath width equal to 0.2 μm has been assumed for the initial conditions in the simulations. Corresponding austenite dimensions are obtained based on the appropriate austenite fraction predicted for every quenching temperature, and the results are shown in Table 2.

Table 1
Mobility ($m^4\ J^{-1}\ s^{-1}$) corresponding to two activation energies and annealing temperatures studied.

Annealing temperature (°C)	Mobility for $Q_M = 180$ kJ mol^{-1}	Mobility for $Q_M = 140$ kJ mol^{-1}
350	2.45×10^{-20}	5.53×10^{-17}
400	2.99×10^{-19}	3.81×10^{-16}

Table 2
Calculated martensite and austenite fractions present at each quenching temperature and corresponding martensite and austenite widths using the constant ferrite width approach.

Quenching temperature (°C)	Approximate fraction at quench temperature		Lath or film width (μm)	
	Austenite	Martensite	Austenite	Martensite
220	0.10	0.90	0.02	0.20
250	0.13	0.87	0.03	0.20
270	0.17	0.83	0.04	0.20
289	0.20	0.80	0.05	0.20
300	0.23	0.77	0.06	0.20
320	0.29	0.71	0.08	0.20
350	0.40	0.60	0.13	0.20
400	0.69	0.31	0.45	0.20

The volume fraction of martensite during annealing can be estimated from the size of the martensite domain at every annealing time. The local fraction of austenite that is stable upon quenching to room temperature is estimated by calculation of the M_s temperature using Eq. (5), presented in Ref. [24], across the austenite carbon profile and by further use of the Koistinen–Marburger [25] relationship to estimate the volume fraction of stable austenite at each point [30]. Final retained austenite fractions are calculated by integration of the area under each local fraction of stable austenite curve for different annealing times [31].

Simulations of the interaction between carbon partitioning and interface migration under the conditions explained above are presented and discussed with respect to the evolution of the phase fractions and phase compositions.

4. Results and discussion

4.1. Carbon profiles in martensite and austenite during annealing

Figs. 2 and 3 show the evolution of carbon profiles in martensite and austenite during annealing at 350 and 400 °C, respectively, assuming a quenching temperature of 300 °C and the three activation energies considered to describe interface mobility. The same figures also show the estimation of the local retained austenite fraction when the material is finally quenched to room temperature after annealing. A general observation is, in all cases, a sharp increase in the carbon content in the austenite close to the martensite–austenite interface at short annealing times.

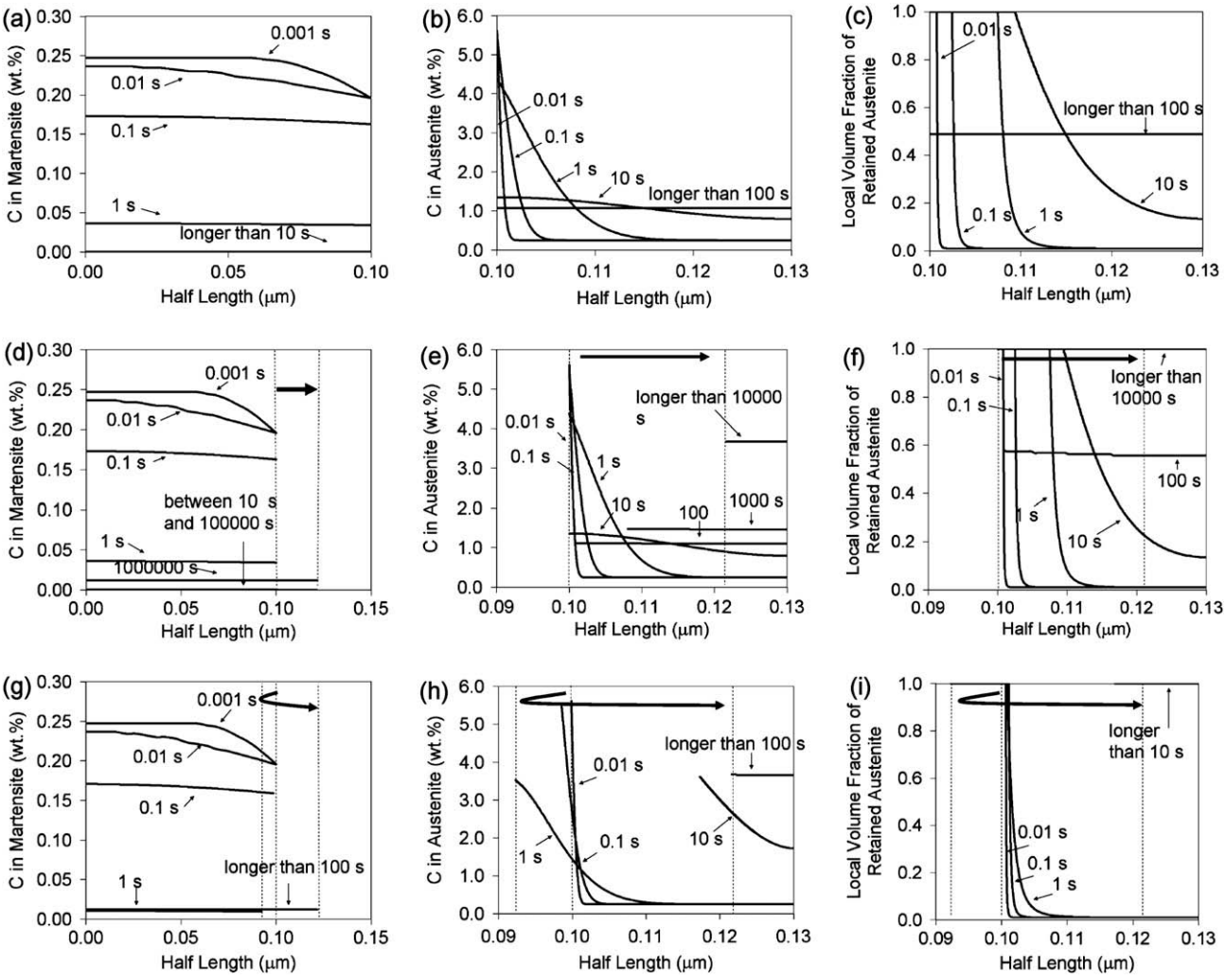

Fig. 2. Calculated carbon profiles in martensite (left column) and austenite (middle column) together with local austenite volume fraction that is stable to the final quench (right column) during annealing at 350 °C after quenching to 300 °C: (a–c) immobile interface; (d–f) $Q_M = 180$ kJ mol^{-1}; (g–i) $Q_M = 140$ kJ mol^{-1}. Arrows in the upper part of the figures and dashed lines indicate the movement of the martensite–austenite interface. According to Table 2, the combined thickness of one martensite plus one austenite film is 0.26 μm when quenching at 300 °C, but because of symmetry the calculation domain includes only the half-thickness, which is 0.13 μm.

Starting with the results corresponding to annealing at 350 °C, it is observed that, under stationary interface conditions (Fig. 2a–c), the sharp carbon profiles observed in the austenite at short annealing times are progressively reduced. After about 100 s, the carbon concentration in both phases is equilibrated according to the conditions established by CCE, i.e. the same chemical potential of carbon in the martensite and the austenite but with the limitation of an immobile interface. Fig. 2c shows estimations of the local fraction of retained austenite, indicating that the final state corresponds to the retention of about half of the austenite available during annealing.

When the activation energy is assumed equal to 180 kJ mol^{-1} (Fig. 2d–f), the interface mobility is not high enough to produce interface migration during the timeframe in which carbon partitioning occurs from the martensite to the austenite. This behavior results in evolution of carbon profiles similar to that obtained with a stationary interface for annealing times lower than 100 s (the time necessary to obtain the final profiles in the case of an immobile interface). However, at longer annealing times, there is interface migration from the martensite into the austenite until the establishment of full equilibrium in both phases, with a substantial reduction of the austenite fraction in this instance. The final profiles are obtained after annealing for about 10,000 s (~3 h). In this case, the volume fraction of retained austenite at the end of the process (Fig. 2f) is less than half of the austenite available after the first quench because of the reduction of the austenite thickness.

When the activation energy is 140 kJ mol^{-1} (Fig. 2g–i), the interface mobility is high enough to produce migration of the martensite–austenite interface during carbon transfer between the two phases. Initially, the carbon content at the interface is higher than the equilibrium value and migration of the interface from the austenite into the mar-

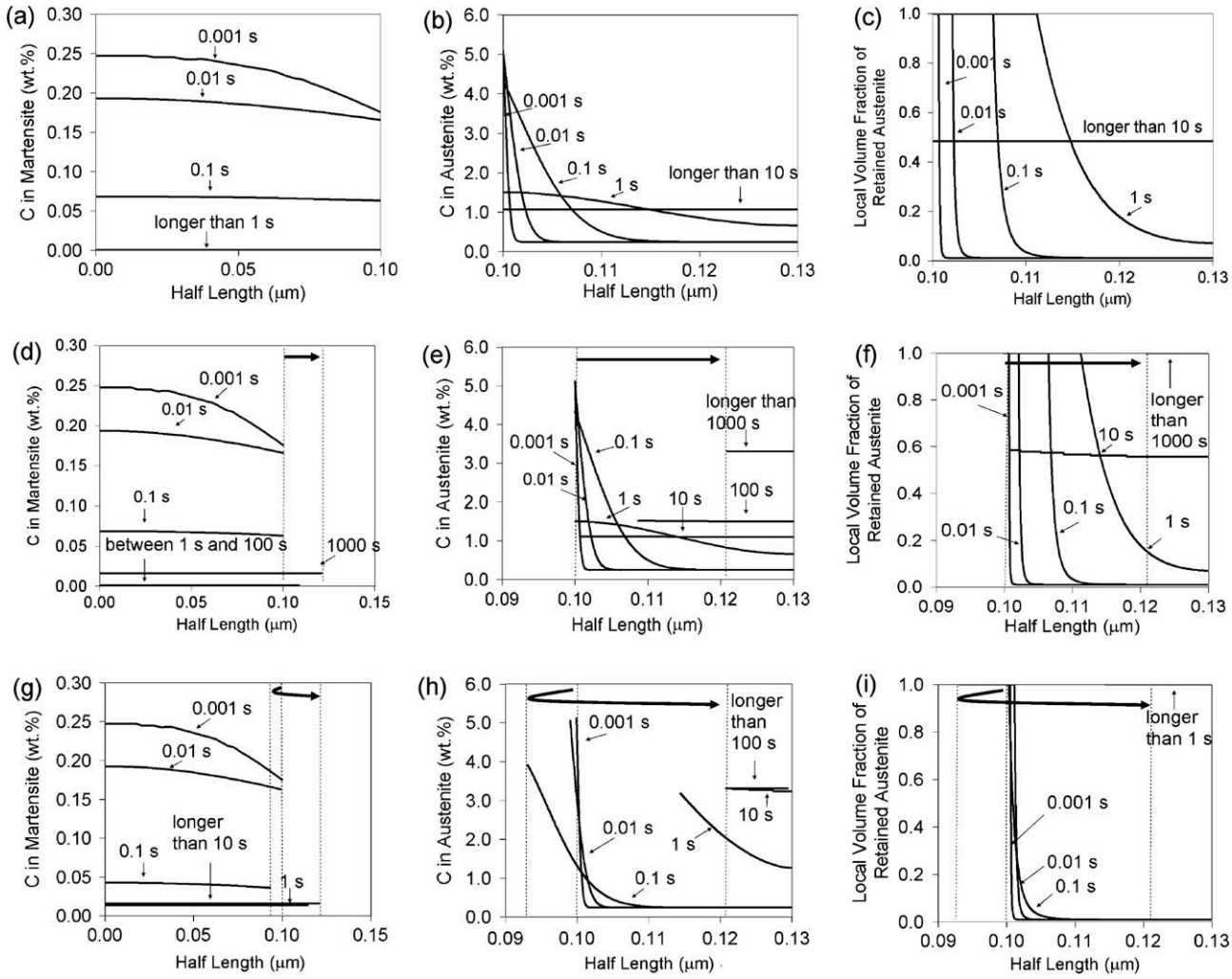

Fig. 3. Calculated carbon profiles in martensite (left column) and austenite (middle column) together with local austenite volume fraction that is stable to the final quench (right column) during annealing at 400 °C after quenching to 300 °C: (a–c) immobile interface; (d–f) $Q_M = 180\ \text{kJ mol}^{-1}$; (g–i) $Q_M = 140\ \text{kJ mol}^{-1}$. Arrows in the upper part of the figures and dashed lines indicate the movement of the martensite–austenite interface. According to Table 2, the combined thickness of one martensite plus one austenite film is 0.26 μm when quenching at 300 °C, but because of symmetry the calculation domain includes only the half-thickness, which is 0.13 μm.

tensite takes place. However, carbon diffusion causes a reduction of this peak in the time interval between 0.1 and 1 s, to carbon levels at the interface that are lower than the equilibrium value. Consequently, the interface then migrates from the martensite to the austenite. The homogenization of carbon in the austenite leads to further movement of the interface until the carbon content corresponding to full equilibrium in both phases is reached after annealing for about 100 s. The time taken to attain the final carbon profiles is similar to the that required in the case of an immobile interface, but considerably lower than for an activation energy of 180 kJ mol^{-1}. The final fraction of local retained austenite (Fig. 2i) is the same as that obtained in the previous case.

From the above results, it is clear that the interface mobility has an important influence on the kinetics of the carbon partitioning process. In the case of a stationary interface or when the interface mobility corresponds to the value determined for reconstructive austenite to ferrite transformations ($Q_M = 140\ \text{kJ mol}^{-1}$), the final carbon profiles are obtained after annealing for a similar length of time (about 100 s). However, in the case of an intermediate interface mobility ($Q_M = 180\ \text{kJ mol}^{-1}$), as might apply to a lower-energy semicoherent interface, the development of the carbon profiles is essentially similar to those obtained in the case of an immobile interface for times shorter than about 100 s. However, longer annealing times lead to slow migration of the interface until full equilibrium conditions are reached after annealing for about 10,000 s.

In the case of annealing at 400 °C (Fig. 3), the evolution of the carbon profiles in martensite and austenite and local fractions of retained austenite is similar to those obtained for annealing at 350 °C, but takes place on a different timescale. For example, uniform carbon concentration profiles in the case of an immobile interface (Fig. 3a and b) and $Q_M = 140\ \text{kJ mol}^{-1}$ (Fig. 3g and h) are obtained in both

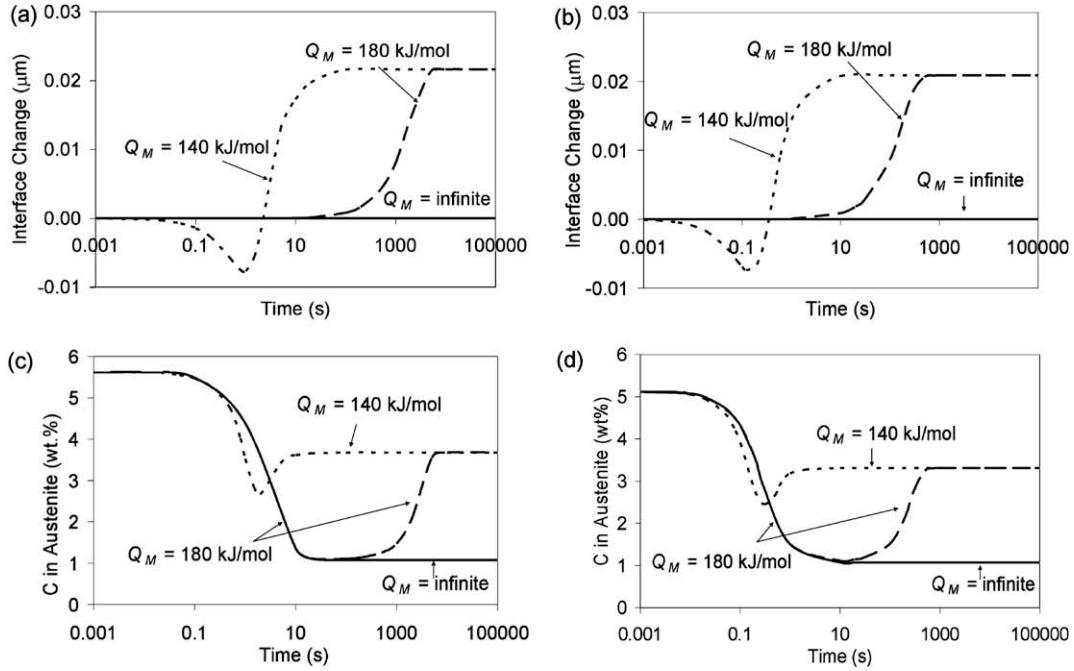

Fig. 4. (a and b) Position of the martensite–austenite interface for quenching to 300 °C and annealing at (a) 350 °C and (b) 400 °C. Position 0.00 refers to the initial position of the interface and any decrease or increase of the position represents a decrease or increase, respectively, of the martensite width. (c and d) Carbon content in the austenite at the interface for quenching at 300 °C and annealing at (c) 350 °C and (d) 400 °C.

phases after annealing for about 10 s. However, in the case of $Q_M = 180$ kJ mol^{-1} (Fig. 3d and e), the time required to reach full equilibrium is substantially longer, in the range between 100 and 1000 s. This is a consequence of the low mobility of the interface.

4.2. Evolution of the interface position during annealing

Fig. 4a and b shows the evolution of the interface position with annealing time for the case of quenching to 300 °C and annealing at 350 and 400 °C, respectively. Fig. 4c and d shows the corresponding evolution of the carbon content in the austenite at the interface. The three curves give results for the three martensite–austenite interface mobilities considered in this work. Examination of these figures leads to the observations described below.

In the case of an immobile interface, the carbon content in the austenite increases fast very early in the process (although this rapid increase in carbon is not represented in the timescale of Fig. 4) and then decreases before reaching the value given by the constrained carbon equilibrium condition. For $Q_M = 180$ kJ mol^{-1}, the interface does not significantly change its position for annealing times lower than about 10 s in the case of annealing at 350 °C and about 1 s for annealing at 400 °C. During this time, the carbon content in the austenite at the interface reaches the value corresponding to CCE, i.e. evolves identically to the case of an immobile interface. However, longer annealing times lead to the initiation of interface migration from the martensite into the austenite and the progressive enrichment of carbon at the interface until full equilibrium conditions are reached. Finally, considering $Q_M = 140$ kJ mol^{-1}, the evolution of the interface position and the carbon concentration in the austenite at the interface largely occur simultaneously during the annealing process. In this case, carbon partitioning starts with an increase of the carbon content in the austenite at the interface, which is compensated by the movement of the interface from the austenite into the martensite. Once the carbon content of the austenite is lower than the equilibrium value, the motion of the interface reverses its direction, from the martensite into the austenite. This migration ends when full equilibrium conditions are reached.

4.3. Evolution of the volume fraction of martensite during annealing

The predicted evolution of the volume fraction[1] of martensite during annealing for the case of quenching to 300 °C and annealing at 350 or 400 °C is shown in Fig. 5. As expected, the volume fraction of martensite for the case of an immobile interface is constant. In the case of $Q_M = 180$ kJ mol^{-1}, the volume fraction of martensite is constant for annealing times below about 100 s (annealing at 350 °C) or 10 s (annealing at 400 °C). Afterwards, the volume fraction of martensite increases by about 0.16. The evolution of the martensite volume fraction with annealing time is more complex for the case of $Q_M = 140$ kJ mol^{-1}. First,

[1] Predicted volume fractions ignore any slight changes in the phase densities associated with carbon partitioning.

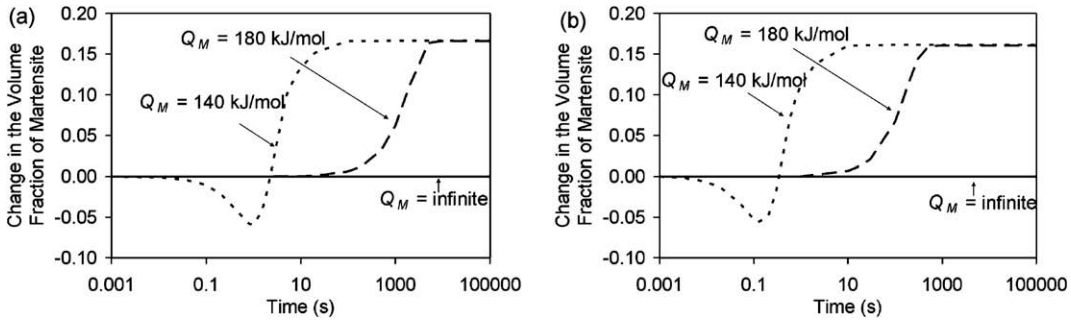

Fig. 5. Simulated evolution of volume fraction of martensite during annealing at (a) 350 °C and (b) 400 °C, after quenching to 300 °C.

the amount of martensite decreases by a volume fraction of about 0.06 below the initial value for both annealing temperatures. The volume fraction of martensite subsequently increases to about 0.16 above the initial value, as in the case of $Q_M = 180$ kJ mol^{-1}. The increase of the volume fraction of martensite predicted in the two latter cases might be consistent with the expansion of the material observed during annealing by some authors [10] and further analysis is suggested to clarify this point.

4.4. Volume fraction of retained austenite after final quench

The volume fraction of retained austenite expected after the final quench to room temperature has been estimated from the local fraction of austenite for every quenching temperature, annealing temperature and time. Predictions are shown in Fig. 6 as a function of the quenching temperature for each interface mobility studied. Similarly, Fig. 7 shows the same results represented as a function of the annealing time.

In the case of an immobile interface (Fig. 6a and d), some interesting features are observed. Firstly, an optimum quenching temperature is obtained where a maximum in the volume fraction of retained austenite is observed. The observation of an optimum quenching temperature is not surprising, since it is a characteristic result of the CCE condition [32]. In the cases analyzed here, this optimum quenching temperature is about 289 °C, associated with a retained austenite volume fraction of 0.20 for both annealing temperatures studied. For quenching temperatures higher than the optimum, the fraction of retained austenite progressively increases with annealing time until it reaches a maximum after annealing for about 10 s (annealing at 350 °C) or 1 s (annealing at 400 °C), and then decreases at longer annealing times. On the other hand, for quenching temperatures lower than the optimum, the fraction of retained austenite increases with time until a maximum value is reached, and no decrease occurs at longer times. Finally, the fraction of retained austenite remains constant for times longer than 100 s (annealing at 350 °C) or 10 s (annealing at 400 °C). These features can be also observed in Fig. 7a and d, which give the fractions of retained austenite as a function of annealing times.

The evolution of the retained austenite fraction with annealing time when $Q_M = 180$ kJ mol^{-1} (Fig. 6b and e) is similar to the behavior observed for the case of an immobile interface for annealing times shorter than about 100 s (annealing at 350 °C) or 10 s (annealing at 400 °C), which represent the point at which the final volume fraction of retained austenite is attained in the case of an immobile interface. In the case of quenching temperatures lower than the optimum (for a stationary interface), the volume fraction of retained austenite progressively decreases at longer annealing times until it reaches the volume fraction corresponding to full equilibrium, as can be also observed in Fig. 7b and e. However, for quenching temperatures higher than this optimum, the volume fraction of retained austenite first increases with annealing time and then decreases before increasing again towards the equilibrium conditions. Here, the volume fraction of retained austenite can show two peaks with annealing time before reaching equilibrium (clearly displayed in Fig. 7b and e). This behavior might offer an explanation for the two peaks reported in the volume fraction of retained austenite observed during annealing by some authors [12]. Full equilibrium conditions are reached after annealing for times up to about 10,000 s (~3 h) at 350 °C, and somewhat earlier at 400 °C.

When an activation energy of 140 kJ mol^{-1} is employed in the simulations (Figs. 6c,f and 7c,f), the evolution of the retained austenite fraction is quite different from the two other cases explained above. In general, for both annealing temperatures and every quenching temperature analyzed, the fraction of retained austenite increases with the annealing time until reaching a maximum which is between 0.07 and 0.12 for the particular alloy used in the simulations, and then decreases to the value corresponding to full equilibrium conditions. As expected, the process is faster for annealing at 400 than at 350 °C.

5. Conclusions

Some aspects of the microstructure evolution in the Q&P process have been considered by means of a modeling approach to analyze processes that may occur during annealing of martensite–austenite grain assemblies. In particular, the influence of interface migration was examined

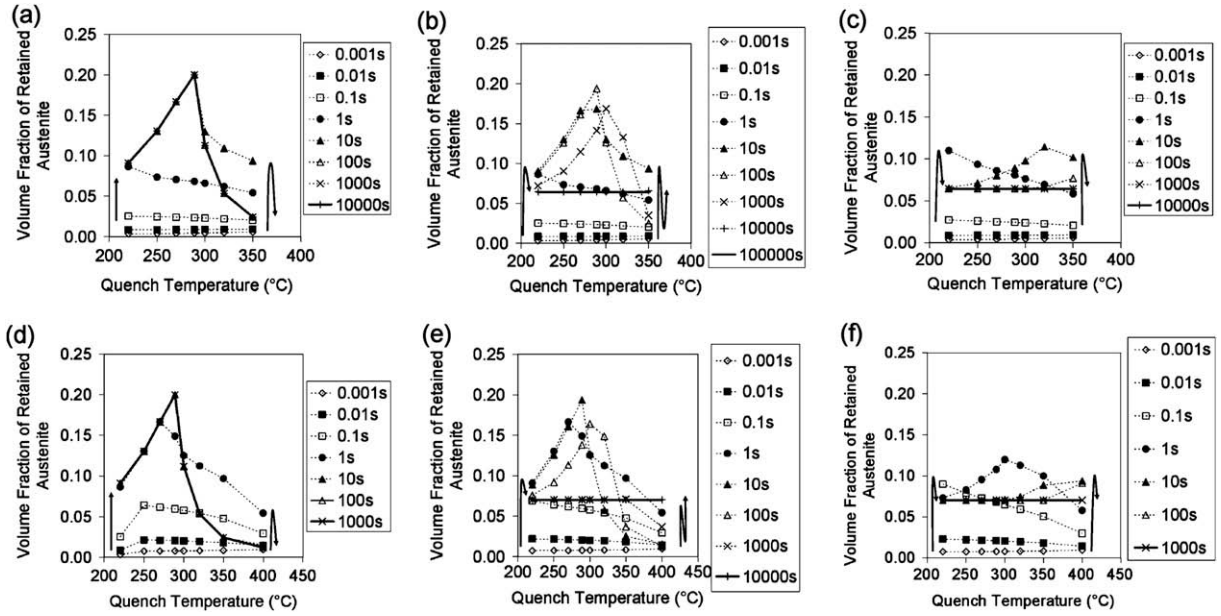

Fig. 6. Results for the volume fraction of retained austenite fraction as a function of the quenching temperature. (a–c) Annealing at 350 °C: (a) stationary interface; (b) $Q_M = 180$ kJ mol^{-1}; (c) $Q_M = 140$ kJ mol^{-1}. (d–f) Annealing at 400 °C: (d) stationary interface; (e) $Q_M = 180$ kJ mol^{-1}; (f) $Q_M = 140$ kJ mol^{-1}. Arrows indicate the evolution of the retained austenite fraction with time for the lowest and highest quenching temperatures studied.

by comparing results computed using different assumptions about interface mobility, ranging from a completely immobile interface (assumed in early Q&P studies) to the relatively high mobility of an incoherent ferrite–austenite interface. An important intermediate case was also considered in an effort to simulate the behavior of a semicoherent martensite–austenite interface. Simulations were made using the assumption that different martensite–austenite interface characters would lead to different activation energies for iron migration. Two different annealing temperatures were studied. The main conclusions obtained from this work can be summarized as follows:

– An infinite activation energy leads to carbon partitioning from martensite to austenite with an immobile interface. The result is equivalent to the behavior reported in

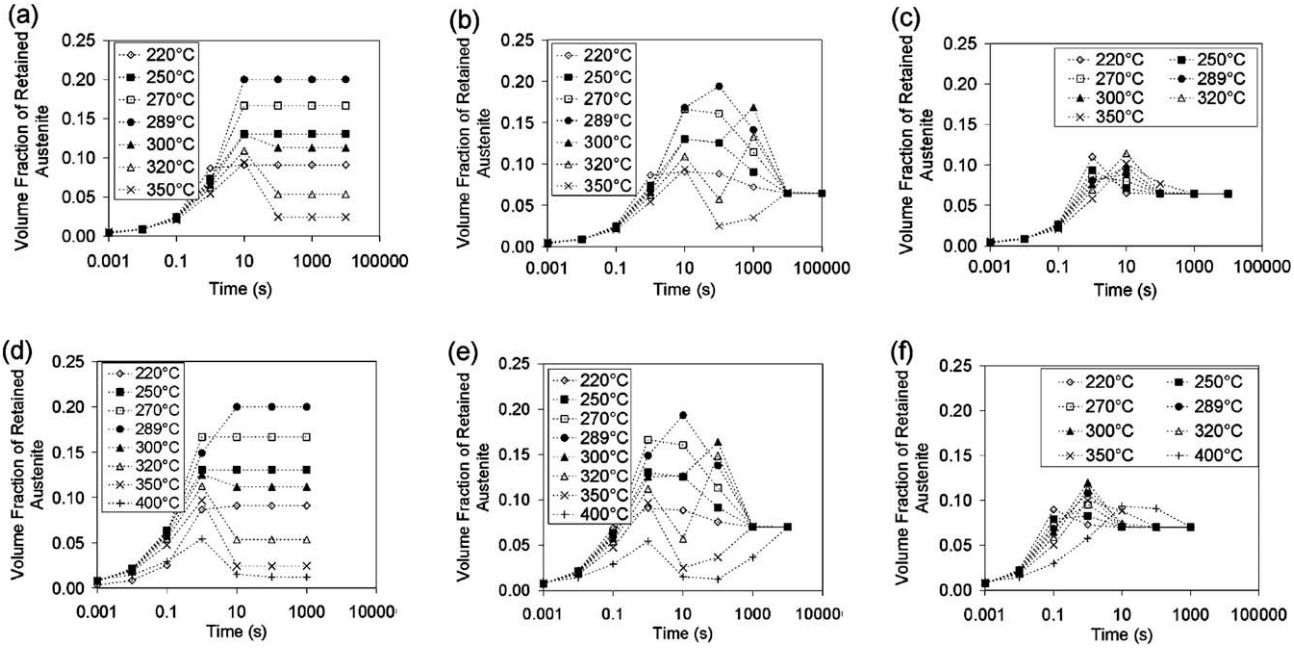

Fig. 7. Predicted volume fraction of retained austenite as a function of the annealing time. (a–c) Annealing at 350 °C: (a) stationary interface; (b) $Q_M = 180$ kJ mol^{-1}; (c) $Q_M = 140$ kJ mol^{-1}. (d–f) Annealing at 400 °C: (d) stationary interface; (e) $Q_M = 180$ kJ mol^{-1}; (f) $Q_M = 140$ kJ mol^{-1}.

the literature for CCE conditions. The evolution of the retained austenite fraction with time is found to be dependent on the quenching temperature. An optimum quenching temperature is predicted (with a maximum in the volume fraction of retained austenite), which is a typical result of the CCE model.

– With an activation energy of 180 kJ mol^{-1}, which is 40 kJ mol^{-1} higher than is typical for reconstructive austenite to ferrite transformation (in order to represent a semicoherent interface), the carbon profiles in both phases are similar to those obtained for the stationary interface during the initial stages of annealing. However, for longer annealing times, the carbon profiles and the volume fractions of phases evolve to full equilibrium conditions. The final carbon content in both phases is independent of the quenching temperature. Examination of the evolution of the volume fraction of retained austenite during annealing for different quenching temperatures has shown that, for quenching temperatures higher than the optimum one (for an immobile interface), two peaks in the retained austenite fraction as a function of annealing time are observed, which might explain some reported experimental observations.
– For an activation energy of 140 kJ mol^{-1}, corresponding to an austenite to ferrite transformation involving incoherent interfaces, carbon partitioning from martensite to austenite and interface migration are coupled during the annealing process, leading to a bidirectional movement of the interface before equilibrium is reached.

The results indicate that different interface mobilities lead to profound differences in the evolution of microstructure that occurs during the annealing of martensite–austenite grain assemblies. Therefore, experimental work to determine the mobility of the martensite–austenite interface will be needed to develop improved models for the prediction of the microstructure evolution during the Q&P process.

Acknowledgments

This research was carried out under the Project No. MC5. 05233 in the framework of the Research Program of the Materials Innovation Institute M2i (www.m2i.nl), the former Netherlands Institute for Metals Research. The authors would like to thank Dr. Dave Hanlon and Dr. Theo Kop (Corus RD&T) for fruitful discussions. The support of Corus RD&T to this project is acknowledged, along with the Advanced Steel Processing and Products Research Center (ASPPRC).

References

[1] Bhadeshia HKDH, Edmonds DV. Metal Sci 1979:325.
[2] Thomas G. Metal Trans A 1978;9A:439.
[3] Speer JG, Streicher AM, Matlock DK, Rizzo FC, Krauss G. In: Damm EB, Merwin M, editors. Austenite formation and decomposition. Warrendale (PA): TMS/ISS; 2003. p. 505–22.
[4] Speer JG, Matlock DK, Edmonds DV. Mater Res 2005;8:417.
[5] Speer JG, Matlock DK, De Cooman BC, Schroth JG. Acta Mater 2003;51:2611.
[6] Speer JG, Matlock DK, De Cooman BC, Schroth JG. Scripta Mater 2005;52:83.
[7] Hillert M, Ågren J. Scripta Mater 2004;50:697.
[8] Hillert M, Ågren J. Scripta Mater 2005;52:87.
[9] Zhong N, Wang X, Rong Y, Wang L. J Mater Sci Technol 2006;22:751.
[10] Kim SJ, Kim HS, De Cooman BC. In: Proc. mater. sci. technol.. Detroit (MI): MS&T; 2007. p. 73–83.
[11] Kim SJ, Speer JG, Kim HS, De Cooman BC. In: International conference on new developments in advanced high-strength steels. Orlando, FL: AIST; 2008. p. 179–89.
[12] Matlock DK, Bräutigam VE, Speer JG. Mater Sci Forum 2003;426–432:1089.
[13] Speer JG, Hackenberg RE, De Cooman BC, Matlock DK. Philos Mag Lett 2007;87:379.
[14] Santofimia MJ, Zhao L, Sietsma J. Scripta Mater 2008;59:159.
[15] Krielaart GP, Van der Zwaag S. Mater Sci Technol 1998;14:10.
[16] Mecozzi MG, Sietsma J, Van der Zwaag S. Acta Mater 2006;54:1431.
[17] Christian JG. The theory of transformations in metals and alloys. 3rd ed. Amsterdam: Elsevier; 2002. p. 961–91.
[18] Thermo-Calc Software. <http://www.thermocalc.se/>.
[19] Thiessen RG, Richardson IM, Sietsma J. Mater Sci Eng A 2006;427:223.
[20] Thiessen RG. Ph.D. Thesis, Delft University of Technology; 2006. p. 130.
[21] Crank J. The mathematics of diffusion. 2nd ed. Oxford: Oxford Science Publications; 1975. p. 137–59.
[22] Ågren J. J Phys Chem Solids 1982;43:421.
[23] Ågren J. Scripta Metall 1986;20:1507.
[24] Mahieu M, Maki J, De Cooman BC, Claessens S. Metall Mater Trans A 2002;33A:2573.
[25] Koistinen DP, Marburger RE. Acta Metall 1959;7:59.
[26] Clarke A.J. Ph.D. Thesis, Colorado School of Mines; 2006. p. 31–2.
[27] Apple CA, Caron RN, Krauss G. Metall Trans 1974;5:593.
[28] Swarr T, Krauss G. Metal Trans A 1976;7A:41.
[29] Marder AR. Ph.D. Thesis, Lehigh University; 1968.
[30] Clarke A.J. Ph.D. Thesis, Colorado School of Mines; 2006, p. 151.
[31] Clarke A.J. Ph.D. Thesis, Colorado School of Mines; 2006, p. 153.
[32] Speer JG, Edmonds DV, Rizzo FC, Matlock DK. Curr Opin Solid State Mater Sci 2004;8:219.